FERMILAB-PUB-19-158-TD
ACCEPTED
DOI: 10.1103/PhysRevLett.122.027001

Evidence for superconductivity above 260 K in lanthanum superhydride at megabar pressures

Maddury Somayazulu[1,*], Muhtar Ahart[1], Ajay K Mishra[2], Zachary M. Geballe[2], Maria Baldini[2], Yue Meng[3], Viktor V. Struzhkin[2], and Russell J. Hemley[1,*]

[1]*Institute for Materials Science and Department of Civil and Environmental Engineering, The George Washington University, Washington DC 20052, USA*
[2]*Geophysical Laboratory, Carnegie Institution of Washington, Washington DC 20015, USA*
[3]*HPCAT, X-ray Science Division, Argonne National Laboratory, Argonne IL 60439, USA*

Recent predictions and experimental observations of high T_c superconductivity in hydrogen-rich materials at very high pressures are driving the search for superconductivity in the vicinity of room temperature. We have developed a novel preparation technique that is optimally suited for megabar pressure syntheses of superhydrides using modulated laser heating while maintaining the integrity of sample-probe contacts for electrical transport measurements to 200 GPa. We detail the synthesis and characterization, including four-probe electrical transport measurements, of lanthanum superhydride samples that display significant drops in resistivity on cooling over a range of temperatures up to 280 K and pressures of 200 GPa. The experiments are supported by pseudo-four probe conductivity measurements, critical current estimates, and low-temperature x-ray diffraction. We suggest that the transitions represent signatures of superconductivity up to near room temperature in phases of lanthanum superhydride, in good agreement with density functional structure search and BCS theory calculations.

[*]zulu58@gwu.edu, rhemley@gwu.edu

The search for superconducting metallic hydrogen at very high pressures has long been viewed as a key problem in physics [1,2]. The prediction of very high (e.g., room temperature) T_c superconductivity in hydrogen-rich materials [3] has opened new possibilities for realizing high critical temperatures but at experimentally accessible pressures (i.e., below 300 GPa) where samples can be characterized with currently available tools. Following the discovery of novel compound formation in the S-H system at modest pressures [4], theoretical calculations predicted that hydrogen sulfide would transform on further compression to a superconductor with a T_c up to the 200 K range [5,6]. The high T_c of 203 K at 150 GPa in samples formed by compression of H_2S was subsequently confirmed [7,8], with x-ray measurements consistent with cubic H_3S as the superconducting phase [9].

Given that the higher hydrogen content in many simple hydride materials is predicted to give still higher T_c values [3], we have extended our studies to higher hydrides, the so-called superhydrides, XH_n with $n > 6$. Systematic theoretical structure searching in the La-H and Y-H systems reveals numerous hydrogen-rich compounds with strong electron-phonon coupling and T_c in the neighborhood of room temperature (above 270 K) [10] (see also Ref. [11]). Of these superhydrides, LaH_{10} and YH_{10} have a novel clathrate-type structure with 32 hydrogen atoms surrounding each La or Y atom, and T_c near 270 K at 210 GPa for LaH_{10} and 300 K at 250 GPa in YH_{10}; see Ref. [12] for a recent review. Notably, in these phases the H-H distances are ~1.1 Å, which are close to those predicted for solid atomic metallic hydrogen at these pressures [13].

Recently, our group successfully synthesized a series of superhydrides in the La-H system up to 200 GPa pressures. Specifically, we reported x-ray diffraction and optical studies demonstrating that the lanthanum superhydrides can be synthesized. The diffraction reveals that La atoms have a face centered cubic (fcc) lattice at 170 GPa upon heating to ~1000 K [14], and a structure with compressibility close that for predicted cubic metallic phase of LaH_{10}. Experimental and theoretical constraints on the hydrogen content give a stoichiometry of $LaH_{10\pm x}$, where x is between +2 and -1 [14]. On decompression, the fcc-based structure undergoes a rhombohedral distortion of the La sublattice to form a structure that has subsequently been predicted to also have a high T_c [13]. Here we report the use of a novel synthesis route for megabar pressure syntheses of such superhydrides using pulsed laser heating and ammonia borane (NH_3BH_3, AB) as the hydrogen source. We detail the synthesis and characterization of several samples of the material using x-ray diffraction and electrical

resistance measurements at 180-200 GPa. The transport measurements reveal a clear resistance drop on cooling at 260 K using four-probe measurements and above 280 K in other experiments. Consistent with low-temperature x-ray diffraction, we infer that the transition is a signature of near room-temperature superconductivity in LaH_{10} and not related to any structural transition.

Samples were prepared using a variety of diamond-anvil cells (DACs), depending on the measurement [16]. For the electrical conductivity measurements, we used a multi-step process with piston-cylinder DACs [15] (Fig. 1). Composite gaskets consisting of a tungsten outer annulus and a cubic boron nitride epoxy mixture (cBN) insert were employed to contain the sample at megabar pressures while isolating the platinum electrical leads [16]. We synthesized the superhydride from a mixture of La and H_2 loaded in the gasket assembly as in our previous work [14], and found that maintaining good contact between the synthesized material and electrodes is not guaranteed. To overcome this problem, we used AB as the hydrogen source [17-19]. When completely dehydrogenated, one mole of AB yields three moles of H_2 plus insulating cBN, the latter serving both as a solid pressure medium and support holding the hydride sample firmly against the electrical contacts (Fig. 1).

The synthesis and structural characterization of samples were carried out *in situ* at high pressure using a versatile diode-pumped ytterbium fiber laser heating system [20] that was adapted for our experiments. In all runs, we observed very good coupling of the laser with the sample and subsequent sharpening of La diffraction peaks; above 175 GPa and temperatures of 1000-1500 K, this resulted in the formation cubic $LaH_{10\pm x}$ [14]. To complete the transformation but avoid the formation of additional phases [16], we needed to maintain sample temperatures below 1800 K. This was achieved by varying the combination of laser power and pulse width of the heating laser. Typically, we found that a 300-ms pulse and a 30-μm laser spot size resulted in optimal transformation and sample coverage, and minimal anvil or electrode damage. Repeated checks on the two-probe resistance between the four electrodes between heating cycles were performed to ensure that electrodes in a given run were not damaged.

Representative diffraction patterns of three samples are shown in Fig. 2, including a $LaH_{10\pm x}$ sample that was verified to have the four-probe geometry intact at 188 GPa (Fig. 1 and Fig. 2c). The characteristic diffraction peaks of $LaH_{10\pm x}$ identified previously in synthesis from La and H_2 are observed, demonstrating that the superhydride phase can indeed be synthesized

from La and AB using the techniques described above. Further, the results show that synthesis can be carried out while maintaining the electrical leads intact. All the samples for which conductivity data are presented were also characterized by x-ray diffraction.

Figure 3 shows electrical resistance measurements as a function of temperature for the sample presented in Fig. 1 at an initial 300 K pressure of 188 GPa. On cooling, the resistance was observed to decrease around 275 K and to drop appreciably at 260 K, as first reported in Ref. [21]. The resistance abruptly dropped by $>10^3$ and remained constant from 253 K to 150 K. Upon warming, the resistance increased steeply at 245 K, indicating the change was reversible but shifted to lower temperature. Upon subsequent warming to 300 K, the pressure was measured to be 196 GPa. We performed no systematic study of the effect of current on the resistance transition in this sample though the sample appeared to degrade with repeated thermal cycling at the higher current level [16]. Since the pressure was not measured as a function of temperature during thermal cycling, the pressure at which the resistance change occurred was not directly determined.

A second four-probe conductivity measurement was carried out at higher pressure (Fig. 4). In this experiment, we performed the synthesis and measured x-ray diffraction and electrical conductivity in-situ within the cryostat on the x-ray beamline. We also more carefully monitored possible changes in T_c with applied current and measured the I-V characteristics in this experiment. At the lowest current (0.1 mA), the sample resistance displays an abrupt drop at 280 K. The transition temperature decreased to 270 K with increasing current of 1 mA and appeared to decrease further at higher currents. Distinct I-V characteristics were observed above and below the transition temperature. The measurements suggest that well into the superconducting phase, $LaH_{10\pm x}$ could exhibit very large critical current densities [16,22]. In this experiment, part of the sample had spread outside the central culet, giving rise to the formation of lower pressure phases with their own transition temperatures. Evidence for high transition temperatures (e.g., >280 K) at the maximum pressure of this experiment was also obtained from measurements on other samples using pseudo-four probe geometries (Fig. S4). Further discussion of these additional experiments is provided in Ref. [16]

An alternative explanation for the resistivity change is a temperature-induced, iso-structural electronic transition with a dramatic increase in conductivity in the low-temperature

phase. Consistent with our previous optical observations [14], the resistance measurements indicate that the high-temperature phase (i.e., normal state) is a metal, so this would be a metal-metal transition. However, calculations reported to date do not predict such a transition within metallic LaH_{10} [10,13]. Nevertheless, low-temperature x-ray diffraction was measured to determine whether the resistance change is due to a temperature-induced structural transition. The x-ray diffraction patterns reveal no structural changes (Fig. S6 and S7) [16].

The complexity of the experiments prevents us from accurately determining the pressure dependence of the possible superconducting T_c, though the highest values (280 K) appear at the highest pressures (200 GPa). We did not attempt to determine the intrinsic resistivity of the superhydride samples because of their complex geometries, and some of the samples are clearly mixed phase, possibly with varying hydrogen stoichiometry [10,16]. In the three-point (pseudo-four probe) geometry, the contact resistance plays a major role and such low resistance values cannot be measured [23,24]. The samples could consist of layers of LaH_x starting from $x = 10$ on the laser heated side and x <10 toward the electrodes. The samples could also have a complicated toroidal geometry consisting of a central region of $LaH_{10\pm x}$ with a peripheral ring of untransformed La arising from the need to preserve the electrodes during laser heating and differential thermal heat transport for the sample in contact with the diamond versus the electrodes. Thus, variability in the observed transition temperatures may also arise from a changing network of the superconducting component on thermal cycling as well as the presence of multiple phases produced within a sample as a result of *P*-*T* gradients during synthesis [16]. Indeed, after our work was completed, a report appeared of possible T_c in lanthanum hydride at 215 K at slightly lower pressure [25], which we suggest may be a signature of another phase [13,16].

In summary, we report four-probe, ac resistance measurements on $LaH_{10\pm x}$ synthesized at pressures of 180-200 GPa by a modulated, pulsed laser heating technique that preserves the integrity of multi-probe electrical contacts on the sample after synthesis. Our multiple measurements reveal the signature of superconductivity at temperatures above 260 K at pressures of 180-200 GPa. The transition temperature is close to that predicted for the superconducting T_c based on BCS calculations for LaH_{10} at comparable pressures. Whereas diamagnetic measurements are needed to confirm the present results, we note the magnitude of the resistance drops repeatedly observed in our experiments is comparable to that observed in previous high-

pressure studies where the transition was subsequently found to be correctly identified as signatures of superconductivity by magnetic susceptibility (e.g., Refs. [23,26]). Extending and applying the latter technique for the smaller and more complex superhydride samples is progress. Infrared, optical, and x-ray spectroscopy [27,28] would also provide useful characterization, including identifying different superconducting phases and establishing the pressure dependence of T_c for each component. The results reported here thus provide the first experimental evidence of conventional superconductivity near room temperature, as exhibited in this new class of hydride materials.

Acknowledgements

We are grateful to H. Liu, S. Sinogeikin, I. I. Naumov, R. Hoffmann, N. W. Ashcroft, and S. A. Gramsch for their help in many aspects of this work. The authors would like to acknowledge the support of Paul Goldey and honor his memory. This research was supported by EFree, an Energy Frontier Research Center funded by the U.S. Department of Energy (DOE), Office of Science, Office of Basic Energy Sciences (BES), under Award DE-SC0001057. The instrumentation and facilities used were supported by DOE/BES (DE-FG02-99ER45775, VVS), the U.S. DOE/National Nuclear Security Administration (DE-NA-0002006, CDAC; and DE-NA0001974, HPCAT), and the National Science Foundation (DMR-1809783). The Advanced Photon Source is operated by the DOE Office of Science by Argonne National Laboratory under Contract DE-AC02-06CH11357.

References

[1] N. W. Ashcroft, Metallic hydrogen - A high-temperature superconductor, *Phys. Rev. Lett.* **21**, 1748 (1968).

[2] V. L. Ginzburg, What problems of physics and astrophysics seem now to be especially important and interesting (thirty years later, already on the verge of XXI century)? , *Phys. Uspekhi* **42**, 353 (1999).

[3] N. W. Ashcroft, Hydrogen dominant metallic alloys: high temperature superconductors?, *Phys. Rev. Lett.* **92**, 187002 (2004).

[4] T. A. Strobel, P. Ganesh, M. Somayazulu, P. R. C. Kent and R. J. Hemley, Novel cooperative interactions and structural ordering in H_2S-H_2, *Phys. Rev. Lett.* **107**, 255503 (2011).

[5] Y. Li, J. Hao, H. Liu, Y. Li and Y. Ma, The metallization and superconductivity of dense hydrogen sulfide, *J. Chem. Phys* **140**, 174712 (2014).

[6] D. Duan, Y. Liu, F. Tian, D. Li, X. Huang, Z. Zhao, H. Yu, B. Liu, W. Tian and T. Cui, Pressure-induced metallization of dense $(H_2S)_2H_2$ with high-T_c superconductivity, *Sci. Rep.* **4**, 6968 (2014).

[7] A. P. Drozdov, M. I. Eremets and I. A. Troyan, Conventional superconductivity at 190 K at high pressures, arXiv:1412.0460.

[8] A. P. Drozdov, M. I. Eremets, I. A. Troyan, V. Ksenofontov and S. I. Shylin, Conventional superconductivity at 203 K at high pressures, *Nature* **525**, 73-76 (2015).

[9] M. Einaga, M. Sakata, T. Ishikawa, K. Shimizu, M. I. Eremets, A. P. Drozdov, I. A. Troyan, N. Hirao and Y. Ohishi, Crystal structure of the superconducting phase of sulfur hydride, *Nature Phys.* **12**, 835-838 (2016).

[10] H. Liu, I. I. Naumov, R. Hoffmann, N. W. Ashcroft and R. J. Hemley, Potential high-T_c superconducting lanthanum and yttrium hydrides at high pressure, *Proc. Natl. Acad. Sci. U.S.A.* **114**, 6990-6995 (2017).

[11] F. Peng, Y. Sun, C. J. Pickard, R. J. Needs, Q. Wu and Y. Ma, Hydrogen clathrate structures in rare earth hydrides at high pressures: Possible route to room-temperature superconductivity, *Phys. Rev. Lett.* **119**, 107001 (2017).

[12] T. Bi, N. Zarifi, T. Terpstra and E. Zurek, The search for superconductivity in high pressure hydrides, arXiv:1806.00163.

[13] H. Liu, I. I. Naumov, Z. M. Geballe, M. Somayazulu, J. S. Tse and R. J. Hemley, Dynamics and superconductivity in compressed lanthanum superhydride, *Phys. Rev. B* **98**, 100102(R) (2018).

[14] Z. M. Geballe, H. Liu, A. K. Mishra, M. Ahart, M. Somayazulu, Y. Meng, M. Baldini and R. J. Hemley, Synthesis and stability of lanthanum superhydrides, *Angew. Chem. Inter. Ed.* **57**, 688-692 (2018).

[15] H. K. Mao, R. J. Hemley and A. L. Mao, Recent design of ultrahigh-pressure diamond cell, in *High Pressure Science and Technology --1993*, edited by S. C. Schmidt*, et al.* (AIP Press, New York, 1994), pp. 1613-1616.

[16] Supplementary Materials.

[17] R. S. Chellappa, M. Somayazulu, V. V. Struzhkin, T. Autrey and R. J. Hemley, Pressure-induced complexation of NH_3BH_3–H_2, *J. Chem. Phys.* 224515 (2009).

[18] Y. Song, New perspectives on potential hydrogen storage materials using high pressure, *Phys. Chem. Chem. Phys.* **15**, 14524–14547 (2013).

[19] R. G. Potter, M. Somayazulu, G. D. Cody and R. J. Hemley, High pressure equilibria of dimethylamine borane, dihydridobis(dimethylamine)boron(III) tetrahydridoborate(III), and hydrogen *J. Phys. Chem. C* **118**, 7280-7287 (2014).

[20] Y. Meng, G. Shen and H. K. Mao, Double-sided laser heating system at HPCAT for in situ x-ray diffraction at high pressures and high temperatures, *J. Phys. Cond. Matter* **18**, S1097 (2007).

[21] R. J. Hemley, Progress on hydride, superhydride, and hydrogen superconductors, *International Symposium: Pressure and Superconductivity. Fundacion Ramon Areces - Madrid, Spain, May 21-22, 2018;* https://www.fundacionareces.tv/watch/superconductividad?as=5b485ea9fe7e8150088b45fe.

[22] J. P. Rush, C. J. May-Miller, K. G. B. Palmer, N. A. Rutter, A. R. Dennis, Y. H. Shi, D. A. Cardwell and J. H. Durrell, Transport in bulk superconductors: a practical approach?, *IEEE Trans. Appl. Superconductivity* **26**, 1-4 (2016).

[23] V. V. Struzhkin, M. I. Eremets, W. Gan, H. K. Mao and R. J. Hemley, Superconductivity in dense lithium, *Science* **298**, 1213-1215 (2002).

[24] A. M. Schaeffer, S. R. Temple, J. K. Bishop and S. Deemyad, High-pressure superconducting phase diagram of ^{6}Li: Isotope effects in dense lithium, *Proc. Nat. Acad. Sci.* **112**, 60-64 (2015).

[25] A. P. Drozdov, V. S. Minkov, S. P. Besedin, P. P. Kong, M. A. Kuzovnikov, D. A. Knyazev and M. I. Eremets, Superconductivity at 215 K in lanthanum hydride at high pressures, arXiv:1808.07039.

[26] R. Dias, C. S. Yoo, V. V. Struzhkin, M. Kim, T. Muramatsu, T. Matsuoka, Y. Ohishi and S. Sinogeikin, Superconductivity in high disordered dense carbon disulfide, *Proc. Nat. Acad. Sci. U.S.A.* **110**, 11720-11724 (2013).

[27] I. Troyan, A. Gavriliuk, R. Rüffer, A. Chumakov, A. Mironovich, I. Lyubutin, D. Perekalin, A. P. Drozdov and M. I. Eremets, Observation of superconductivity in hydrogen sulfide from nuclear resonant scattering, *Science* **351**, 1303-1306 (2016).

[28] J. P. Carbotte, E. J. Nicol and T. Timusk, Detecting superconductivity in the high pressure hydrides and metallic hydrogen from optical properties, *Phys. Rev. Lett.* **121**, 047002 (2018).

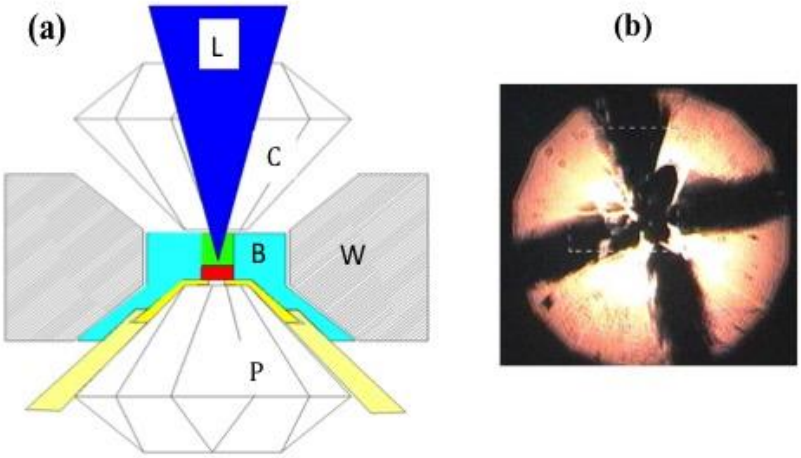

Figure 1. (a) Schematic of the assembly used for synthesis and subsequent conductivity measurements. The sample chamber consisted of a tungsten outer gasket (W) with an insulating cBN insert (B). The piston diamond (P) was coated with four 1-μm thick Pt electrodes which were pressure-bonded to 25-μm thick Pt electrodes (yellow). The 5-μm thick La sample (red) was placed on the Pt electrodes and packed in with ammonia borane (AB, green). Once the synthesis pressure was reached, single-sided laser heating (L) was used to initiate the dissociation of AB and synthesis of the superhydride. To achieve optimal packing of AB in the gasket hole, we loaded AB with the gasket fixed on the cylinder diamond (C). (b) Optical micrograph of a sample at 178 GPa after laser heating using the above procedure (sample A).

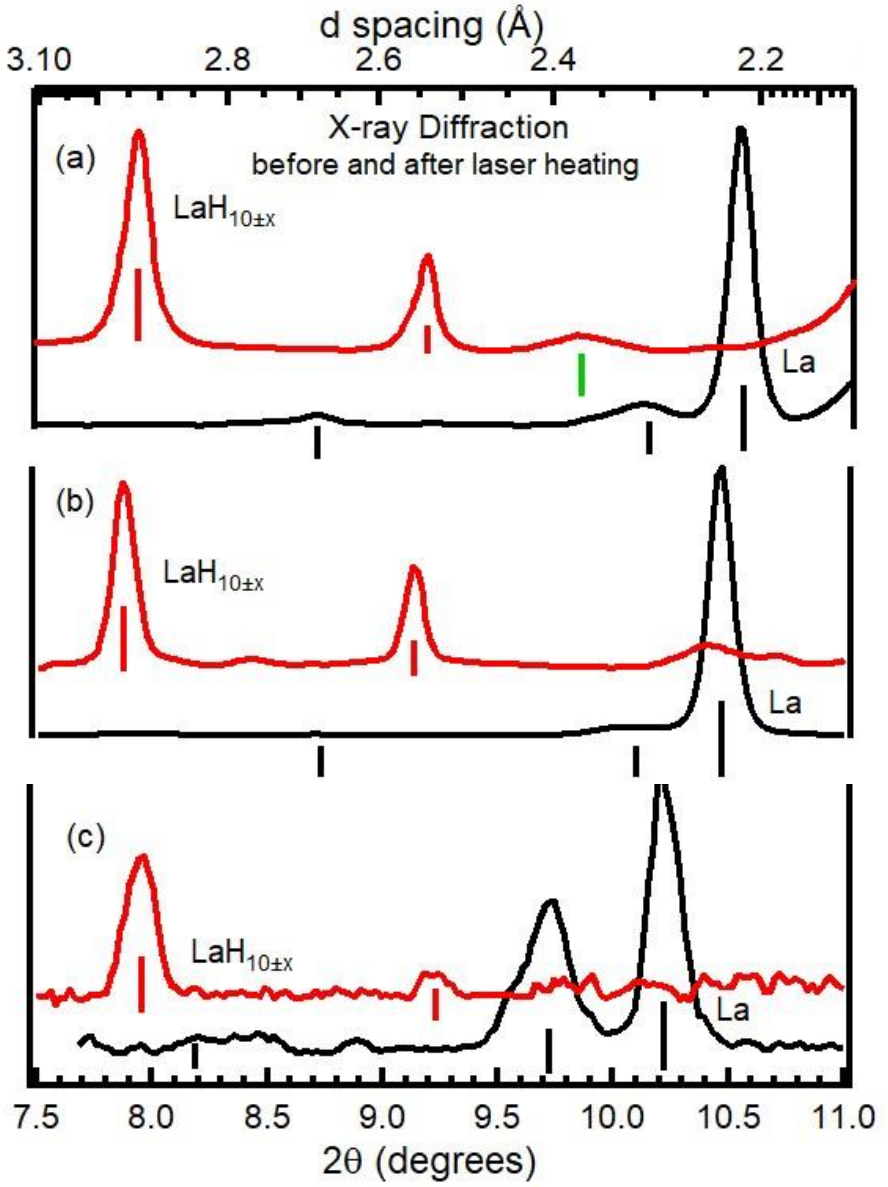

Figure 2. Synchrotron x-ray diffraction patterns obtained from three samples in which $LaH_{10\pm x}$ was synthesized by laser heating at pressures above 175 GPa. (a) X-ray diffraction following laser heating of a mixture of La and H_2 (Au pressure marker); (b) and (c) results obtained following laser heating of La and NH_3BH_3 (Samples A and C, ref [16]; Pt pressure marker). The data were obtained from three separate runs with a nominal x-ray spot size of 5 x 5 μm. In all three panels, the pattern in black is from unreacted La, and that in red is fcc-based $LaH_{10\pm x}$ obtained after laser heating. The sample shown in (c) was nominally 5-μm thick and shows a high degree of anisotropic stress, as indicated by the relative intensities, broadening, and shift of the La peaks prior to the reaction. The diffraction peak marked by the green symbol in (a) is residual WH_x, which is formed when H_2 is present; this hydride also gives rise to the tail above 10.5 degrees. WH_x features are absent in the other two patterns because of the use of insulating cBN gaskets. Further details are provided in Ref. [16].

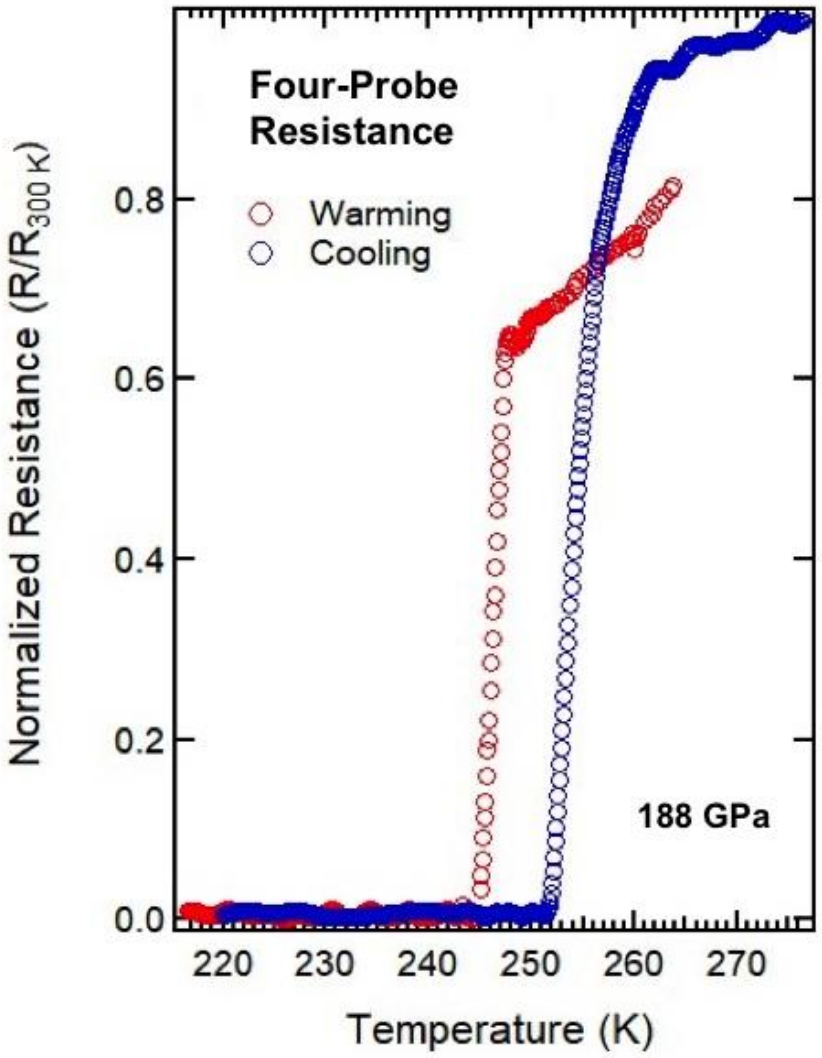

Figure 3. Normalized resistance of the $LaH_{10\pm x}$ sample characterized by x-ray diffraction and radiography (Figs. 1 and 2) and measured with a four-probe technique (sample A, ref [16]). The initial pressure determined from Raman measurements of the diamond anvil edge was 188 GPa. The lowest resistance we could record was 20 μΩ whereas the 300 K value was 50 mΩ. The measurements were performed at 10 mA and 10 kHz.

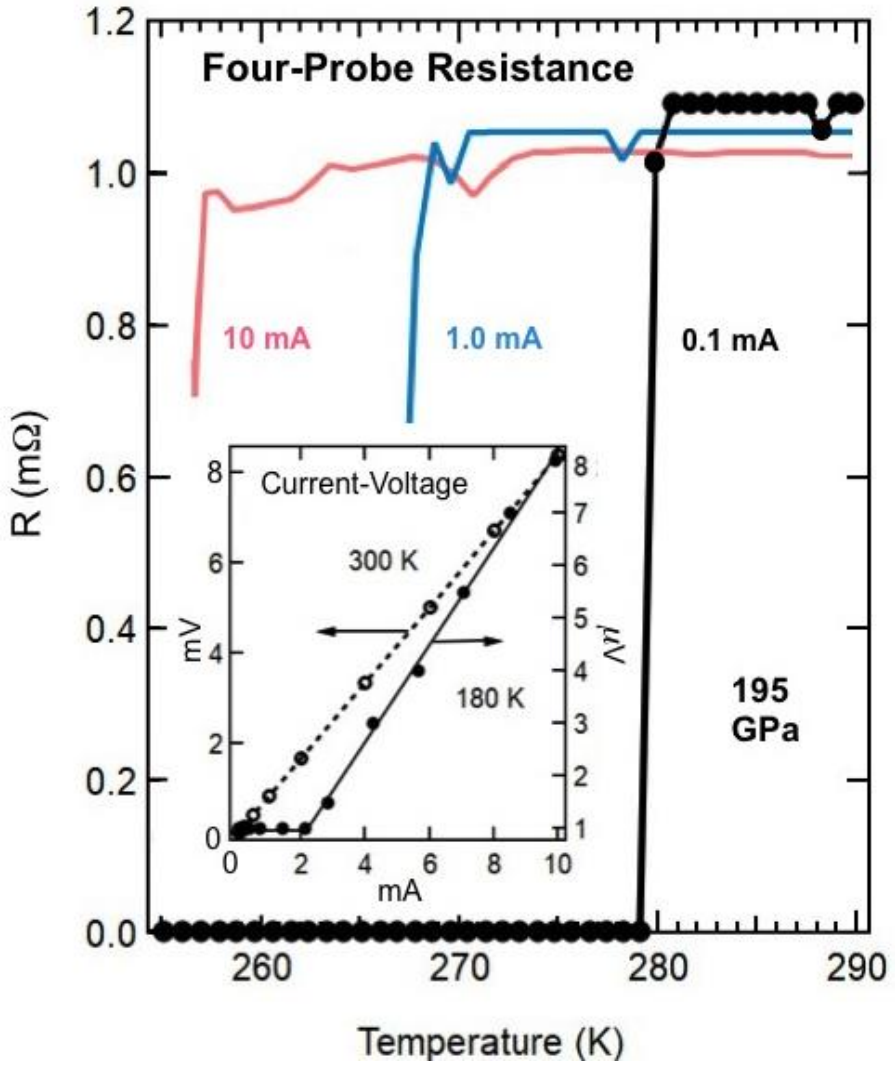

Figure 4: Measurement of resistance using the four-probe technique (Sample F; see Ref. [16]). At the lowest current of 0.1 mA, the sample resistance displays an abrupt drop at 280 K (black curve with symbols, first heating cycle). The transition temperature decreases with increasing current, as shown for 1 mA (blue curve, third heating cycle) and 10 mA (red curve, fifth heating cycle). The inset shows I-V curves obtained from this experiment, and compare data measured at 300 K with measurements well below the transition temperature (180 K). In contrast to those presented in Fig. 3, these measurements were made *in-situ* on the synchrotron station and we were forced to use an internal heater to accelerate the sample warming and correspondingly smaller density of temperature data was obtained (see SM for more details).

Supplementary Materials

Evidence for superconductivity above 260 K in lanthanum superhydride at megabar pressures

Maddury Somayazulu[1,*], Muhtar Ahart[1], Ajay K Mishra[2], Zachary M. Geballe[2], Maria Baldini[2], Yue Meng[3], Viktor V. Struzhkin[2], and Russell J. Hemley[1,*]

[1]*Institute for Materials Science and Department of Civil and Environmental Engineering, The George Washington University, Washington DC 20052, USA*

[2]*Geophysical Laboratory, Carnegie Institution of Washington, Washington DC 20015, USA*

[3]*HPCAT, X-ray Science Division, Argonne National Laboratory, Argonne IL 60439, USA*

[*]zulu58@gwu.edu, rhemley@gwu.edu

Overview

We have developed a novel preparation technique that is optimally suited for megabar pressure syntheses of superhydrides using pulsed laser heating while maintaining the integrity of sample-probe contacts for electrical transport measurements to 200 GPa. We report the synthesis and characterization, including four-probe electrical transport measurements, of lanthanum superhydride samples that display a significant drop in resistivity on cooling. In this supplementary material, we include additional details on pressure measurements, analyses of electrical conductivity data, low-temperature x-ray diffraction, measurements on polyphase samples, and discussion of the critical current densities.

Table S1 lists the samples for which results are presented in this study. The synthesis pressures listed include those based on the diamond Raman [1], and Pt [2] and Au [3] x-ray diffraction scales. The cell volumes listed for lanthanum superhydride are the volume per formula unit based on the position of the 111 diffraction peak assuming a cubic (*Fm*-3*m*) structure. For pure La, the positions of the two strongest peaks, which are assigned to the 113

and 024 lines of a distorted fcc (*hR*24) structure [4], were used to determine the cell volume. Additional x-ray diffraction data on La, together with refinements of the structure and its evolution to these pressures, is described elsewhere [5].

General Sample Preparation

Lanthanum metal (99% purity) was obtained from Goodfellow Metals, opened and stored in a glovebox with flowing Ar atmosphere having low O_2 and H_2O content of <0.1 ppm and <1 ppm, respectively. Reaction with air to form an oxide layer on the sample is expected; indeed, when extracting 5-10 μm samples, unless appropriate care is taken, substantial part of the loaded sample would be an oxide. To address this, we loaded the sample either inside the glovebox or loaded within 30 mins of removal from the glovebox. The purity of the La determined from electron microprobe analysis gave values of 1.7 wt% oxygen, and no other metal impurities were detected (indicative that the overall purity of the sample was as quoted by the supplier). For every loading, we also sheared the La foil with the diamond anvils inside the glovebox, which both thinned down the foil as well as removed possible contaminates to expose a shiny, metallic surface. These pieces were then carefully selected under a microscope attached to the glovebox and transported onto another pair of anvils, which were used to further compact the sample.

For experiments with ammonia borane (NH_3BH_3, AB) as the hydrogen source, one half of the cell (usually the cylinder part which had the gasket glued onto the diamond, was loaded with AB and kept strictly inside the glovebox since this compound is extremely air-sensitive. The La sample was positioned precisely on top of the electrodes outside the glovebox using a micromanipulator within 30 minutes of the removal from the glovebox. The DAC was clamped inside the glovebox and pressure typically raised to about 60 GPa. In all the gas loading runs, including those described in our previous work [4], the cells were first closed in the glovebox with the La metal loaded and subsequently opened once inside the gas loader to trap the densified gas (i.e., at pressures close to 0.2 GPa).

Anvils for electrical conductivity measurements were prepared using a multi-step process using standard piston-cylinder DACs [6]. Four Pt probes were sputtered onto the piston diamond (after a Ti adhesion layer was first deposited) and connected to the external wires using a combination of 25-μm thick Pt ‘shoes’ soldered onto brass holders. We used double

beveled anvils to minimize the loss of electrical contacts due to shearing of the intermediate connections at the gasket-diamond interface. We used 0.3 carat anvils with a 45-60 μm central culet beveled to 250 μm at 9° and to 450 μm at 8°. Compound gaskets consisting of a W outer annulus and a cubic boron nitride (cBN) insert were employed to encapsulate the sample at megabar pressures while isolating the electrical leads. In a typical run, a 5-μm thick sample of La was sandwiched between the electrodes and AB (typically 5-8 μm thick) in a cBN sample chamber about 40 μm in diameter. When pressure was increased, the rapid compression of the softer AB caused the cBN sample chamber to thin rapidly. We found that an initial cBN gasket thickness less than 15 μm guaranteed no implosion of the gasket, which would in turn compromise the electrodes.

X-ray Diffraction and Laser Heating

After loading, synchrotron x-ray diffraction of the La-AB mixture was measured on beamline 16-ID-B of Sector 16, HPCAT at the Advanced Photon Source, Argonne National Laboratory. Typically, a 5 x 5 μm focused x-ray beam at 0.4066 Å was rastered across the sample (Fig. S1). This served as both the check on the chemical integrity of the sample as well as determining the spatial extent over which laser heating needed to be performed for synthesis. As in the previous experiments using H_2 gas as a hydrogen source [4], there was no evidence for reactions with the La during compression without heating. Further, no appreciable peak broadening occurred on compression, indicating that AB served as a reasonably quasihydrostatic pressure medium, though less so than pure H_2 as mentioned below. Pressure was determined using x-ray diffraction from the Pt electrode at the anvil tip Pt [2] and in some cases a Au pressure marker [3], and cross-checked with that determined from the Raman shift of the diamond anvil edge with 660 nm and 532 nm laser sources [1]. The observed compression of the La sample determined by x-ray diffraction was found to coincide with a control run using Ne as a pressure medium (Fig. S2) [4], further confirming that AB exhibits similar quasi-hydrostaticity at these conditions.

Our synchrotron powder x-ray diffraction data on La with Ne, H_2 and AB all show that above 60 GPa, La remains in a distorted fcc (*hR*24) or closely related phase to 180 GPa. Early high-pressure x-ray studies of La using energy dispersive techniques suggested that La transforms to the fcc phase near 60 GPa [7]. However, direct comparison of our data with the

lower resolution patterns presented in Ref. [7] at similar pressures (Fig. S2) shows that the data are not inconsistent. Indeed, laser heating La near 100 GPa in the absence of the hydrogen source, the material remains in a distorted fcc phase with only changes in the relative intensities of some of diffraction peaks occurring, as shown for heating near 100 GPa in Fig. S2. Structure systematics for rare earth elements suggest that La could transform to other structures at these pressures such as a monoclinic *C*2/m structure [8-10]. Our x-ray data are not consistent with such a transition occurring at the conditions of our experiments. Should such a transition occur (perhaps partially), the resulting structure would have volume within 2% of *hR*24 (see also Ref. [8]). Such a shift is within the symbol size (error bar) of the La data plotted in Fig. S3 and would not affect our conclusions regarding the synthesis and characterization of $LaH_{10\pm x}$, which is the focus of this paper. Discussion of the structure of La at megabar pressures, including additional analyses of La data presented in Ref. [4], will be presented elsewhere [5].

Pulsed laser heating was used to reduce damage to the anvils as well as to minimize formation of other reaction products mentioned below. Only single-sided laser heating was performed since the synthesis proceeded from the La-AB interface, and this was the side that is buffered from both the diamond and the electrodes [11]. The laser spot size was typically kept to roughly 30 μm to match the sample and minimize heating of the electrodes. Chilled water was circulated around the cell to minimize movement due to thermal expansion of assembly components. This cooling was crucial since movement of the cell would result in changes in laser alignment and/or laser spot size that could damage the electrodes. The sample was rastered in the x-ray beam following the laser heating to confirm complete transformation. Typically, we found that the region in contact with the electrodes could be partially transformed, which is plausible since the electrodes would act as an additional heat sink with which the sample is in thermal contact.

Depending on the peak temperature, the heating laser pulse width, the thickness of the La sample, and the gasket thickness (which dictates the La to AB ratio), we synthesize a structure consistent with $LaH_{10\pm x}$. Above 2000 K, we observed additional diffraction peaks, including those indicating a monoclinic unit cell similar to that reported for $Mg(BH_2)_2$. In certain experiments, we found that the sample extruded from the central culet thereby resulting in a sample with pressure gradients up to 40 GPa. In such situations, although the heating is

performed on the central part, thermal conductivity results in heating of the La metal in contact with AB at lower pressures. X-ray diffraction of such samples indicated formation of substoichiometric $LaH_{10\pm x}$ (e.g., $x < -1$) and sometimes a mixture of rhombohedral and cubic phases [4]. This would obviously result in a multiphase sample and correspondingly the electrical transport measurements reflect multiple transition temperatures.

The observed successful synthesis of the lanthanum superhydride from AB is consistent with prior work on the hydrogen storage material. Although there is limited experimental data on the behavior of AB above 50 GPa, our extensive earlier studies of the *P*-*T* dependence of dehydrogenation in AB (and related compounds by other groups) under pressure indicate both release of H_2 and no subsequent uptake of H_2 after release at high pressures [12-14]. In addition, reports of catalytic dehydrogenation of AB presents the possibility of enhanced chemical activity at the La-AB interface [15].

In our previous work, we constrained $\pm x$ to be between +2 and -1 [4]. On cooling, samples A-C all exhibit abrupt resistance drops beginning as high as 280 K, whereas the resistance in sample D (untransformed La) monotonically decreases, characteristic of a normal metal. The resistance in the two samples denoted by open symbols were also measured but displayed no abrupt resistance drops on cooling, despite the fact that the four probes for both remained intact after synthesis. The diffraction data thus indicate that samples A, B, C, and E have substoichiometric hydrogen (Fig. S3). The volumes were estimated assuming a cubic structure, i.e., assuming the strongest diffraction lines are cubic 111 and 200, but a distortion of the structure found previously by x-ray diffraction [4] and predicted theoretically [16], cannot be ruled out. The samples corresponding to the points below the $La + 4H_2$ line did not show the resistivity transition in temperature scans down to 150 K.

Electrical Conductivity Measurements

For samples A-D, after synthesis the DACs were mounted in a flow-type cryostat (i.e., off-line from the x-ray measurements), and the leads connected to a function generator and lock-in amplifier for the electrical conductivity measurements [17]. Pressures were monitored from room-temperature diamond Raman measurements after each cooling and warming cycle. Pressure shifts during cooling cycles were minimized by using opposing load screws, though for stainless steel piston-cylinder cells, pressures tend to increase during the first cooling cycle by

as much as 10 GPa. Electrical conductivity of samples F and G were measured following synthesis on the x-ray beamline, as described below.

Our lock-in amplifier technique is able to measure down to the nΩ range, which would be sufficient for conventional macroscopic samples. However, measurements on very small samples at megabar pressures in DACs, especially samples synthesized in situ by laser heating, present several issues. The lowest measurable resistance in our experiments was dictated by noise generated from inductive coupling between probes as well as the complicated geometry expected from a slab consisting of partially transformed $LaH_{10\pm x}$, especially at the edges in contact with the electrical leads. We bracketed this noise from control measurements on samples of elemental copper with aspect ratios similar to those of our samples; these measurements were cycled over a similar temperature range. We used the observed noise levels as a measure of our lowest recordable resistance. Measurements conducted over many temperature cycles indicated a value of 20 $\mu\Omega$ as an approximate lowest bound based on the observed noise level.

The results of two four-probe experiments are presented in the main text. Figure 4 shows that increasing the currents shifts the transition to lower temperature. By measuring four-point voltage on sample F using currents from 0.1 to 10 mA, we can also obtain an initial estimate of critical current density of the superconducting phase. These estimates are limited in accuracy by uncertainty in the dimensions of superconducting phase and by the relatively coarse sensitivity of our electrical field measurements, a result of studying samples of small dimensions buried within the DAC. Well below T_c, four-point voltage increases steadily from its baseline at I > 2 mA. This corresponds to a critical current density of at least ~5000 A/cm^2, given that the maximum cross sectional area of our sample is approximately 40 μm^2. Such a critical current density would generate an electric field of >250 μV/cm (1 μV/40 μm sample), which is significantly larger than that typically used to define the critical current of a bulk superconductor at ambient pressure (e.g., the 1 μV/cm criterion of Ref. [18]). Further experiments are needed to refine these initial estimates. We also point out that application of high ac currents of 10 mA in the two four-probe experiments (samples A and F) resulted in partial degradation of the sample and abnormal variations in measured resistance as a function

of temperature. Additional experiments and modeling efforts are underway to understand this behavior.

Additional experiments were conducted using a three-point (pseudo four-probe) geometry. In these measurements, the observed resistance is a sum of the sample resistance and the contact resistance (e.g., Refs. [19,20]). The normalized resistance is defined as R(T)-R_c(T)/R(300 K)-R_c(T), where R_c is a linear fit to resistance at temperatures below the transition extrapolated to temperatures above the transition. The estimated contact resistance as a function of temperature R(300 K) is the ambient temperature resistance of $LaH_{10\pm x}$ (sample B). This is plotted in Fig. S4 along with the resistance of unreacted La (sample D). The pressure measured at room temperature with the diamond Raman gauge [3] increased gradually with every cooling and warming cycle, as determined from measurements performed after the sample was extracted from the cryostat. The results suggest an increase in T_c with pressure, but direct measurements of the pressure at low temperature are required to confirm this.

An example of steps used in correcting for the contact resistance and obtaining the normalized sample resistance as a function of temperature are shown in Fig. S5 for sample B. As is evident from the second panel, this ratio drops at about 250 K and shows a linear decrease thereafter. We assume that the linear resistance below this drop arises from residual contact resistance. The latter is subtracted from the whole curve to produce the curve in the lowest panel, i.e., the relative resistance corrected for a contact resistance. The same procedure was applied to the other measurements made on this sample (B) shown in Fig. S5.

Low-Temperature X-ray Diffraction

The sample studied with X-ray diffraction at 80 to 300 K was synthesized from La and AB as described above, but without electrodes, an insulating gasket, a non-magnetic DAC [21]. The results of the low-temperature x-ray diffraction results are shown in Figs. S6 and S7. Due to the large 'footprint' of the cryostat (a flow type L-N_2 cryostat equipped with sapphire windows), a beam defining, collimating pinhole could not be placed close to the sample and correspondingly, a larger incident beam interrogated several parts of the sample at the same time. Further, due to differential contraction of several components in the cryostat, it is very difficult to interrogate the exact same part of the sample at different temperatures. We therefore

obtained several diffraction patterns across a 50 x 50 μm grid (in 10-μm steps) and analyzed all of them.

The data were fitted with several diffraction peaks comprising the sample, the pressure marker and cryostat window. This was a preferred method for extracting the d-spacings of Pt and $LaH_{10\pm x}$ since any profile refinement would not be able to account for pressure distribution as well as sample inhomogeneity. Strong diffraction peaks from components associated with cryostat exit window are observed, which contributes to the uncertainties in the d-spacings (Fig. S7). Nevertheless, the available data do not reveal evidence for any new diffraction indicative a temperature-induced structural transition in the material in the 80 – 300 K temperature interval at 185 GPa. The lines show that there is neither a large pressure drift nor change in the *P*-*V* dependence of $LaH_{10\pm x}$ in this temperature range. In general, our experience with the stainless steel (SS) long piston-cylinder cells equipped with SS spring washers has been that the pressure increases on cooling (at least in the first cycle) by about 10-20 GPa due to changes in washer dimensions and thereby the load. The non-magnetic cell and Be-Cu spring washers used in the low temperature x-ray diffraction experiment typically show smaller pressure drifts due to changes in load [21]..

Mixed Phase Samples

We conclude with additional discussion of the experiments on samples F and G. These experiments were performed both to explore behavior with smaller diamond culets and with the sample synthesis, x-ray diffraction and electrical conductivity measurements conducted in situ in a cryostat on the x-ray beamline. The same La + AB synthesis route described above was used in a sample chamber compressed between 45 μm culets using a non-magnetic DAC [21]. The smaller culets generate higher pressures as well as larger pressure gradients. Both the samples spread out of the culet area with increasing pressure, and were 40-50 μm in size prior to laser heating at the maximum pressure of 180 GPa. This translates to a pressure gradient across the sample of more than 30 GPa as determined by diffraction from the Pt electrodes. The samples therefore constituted of a central region in contact with the electrical contacts at 180 GPa and simultaneously reflected a pressure of 150 GPa in the outer regions of the sample.

The pressure distribution was confirmed by obtaining diffraction of both the untransformed La and Pt diffraction peaks with a 50 x 50 μm grid scan using a 5 x 5 μm x-ray beam and a 10-μm defining pinhole close to the sample. As described above for the other samples, single-sided laser heating was performed on both samples while measuring the evolution of diffraction patterns and temperatures. The appearance of the characteristic 111 and 200 diffraction peaks of the lanthanum superhydride confirmed the synthesis. As expected, the position of the peaks varied across the sample, indicative of the expected pressure gradient. The result also suggested possible compositional gradients (cf., Fig. 3). Unfortunately, the very thin samples (~2 μm) produced with these small diamond culets gave rise to low S/N that precluded determination of whether the resultant phase was cubic or rhombohedral, or even the presence of lower symmetry phases such as those found in our previous experiments [4] and predicted theoretically [16,22,23].

Conductivity measurements on sample F performed while measuring x-ray diffraction *in situ* confirmed the separate low-temperature diffraction measurements that indicated no obvious change in symmetry or volume of the sample on cooling below the transition. A gradual increase in pressure during our first cooling cycle was observed. The pressure at the end of the first cooling cycle was determined to be 190 GPa. Based on our observation that the coupling to the heating laser was optimal outside the culet, we infer that the major part of the sample synthesized was at a lower pressure and had probably lower hydrogen content. The complicated geometry would therefore include regions of different hydrogen stoichiometries.

A comparison of the resistivity behavior of samples A (Fig. 3, main paper) and F (Fig. 4, main paper) shows an apparent difference in the normal state behavior as well as the character of the transition but we attribute these differences to the fact that while sample A is localized on the central culet, sample F has a complex geometry due to having a considerable volume extending beyond the central culet (these regions would be at lower pressures and temperatures during synthesis). Obviously, the difference signifies different ratio of normal/superconducting phase volumes which even micro, x-ray diffraction cannot resolve easily. Modifications are being made to design better sample geometries including thin-film deposition of La metal onto the electrodes.

Sample G showed a very small resistance to start with and a small jump at 240 K on warming. Unfortunately, the electrodes in this sample shorted on the culet (resulting in a starting resistance that was in the μΩ level, which precluded more detailed characterization of this sample. In the experiments on sample F, we observe signatures of at least two major transitions in electrical transport measurements. The first transition occurs above 260 K and there is also a second transition observed around 220 K below which temperature the resistance remains unchanged and near zero. It is for this reason that we chose to obtain the I-V curves below this temperature. After our work was completed, a report appeared of possible T_c in lanthanum hydride at 215 K at slightly lower pressure [24], which we suggest may be a signature of another phase [16]. Indeed, numerous phases in the La-H system are both predicted and observed at megabar pressures [4,22], and the possibility that phases other than cubic LaH_{10} exhibit high temperature superconductivity cannot be ruled out (e.g., Ref. [16]). Additional experiments are underway to identify and characterize these phases, as are Meissner effect measurements using enhancements of megabar magnetic susceptibility techniques [25].

References

[1] Y. Akahama and H. Kawamura, Pressure calibration of diamond anvil Raman gauge to 310 GPa, *J. App. Phys.* **100**, 043516 (2006).

[2] A. Dewaele, P. Loubeyre and M. Mezouar, Equations of state of six metals above 94 GPa, *Phys. Rev. B* **70**, 094112 (2004).

[3] D. L. Heinz and R. Jeanloz, The equation of state of the gold calibration standard, *J. Appl. Phys.* **55**, 885 (1984).

[4] Z. M. Geballe*, et al.*, Synthesis and stability of lanthanum superhydrides, *Angew. Chem. Inter. Ed.* **57**, 688-692 (2018).

[5] M. Somayazulu, Z. M. Geballe, A. K. Mishra, M. Ahart, Y. Meng and R. J. Hemley, Crystal structures of La to megabar pressures, in preparation.

[6] H. K. Mao, R. J. Hemley and A. L. Mao, Recent design of ultrahigh-pressure diamond cell, in *High Pressure Science and Technology --1993*, edited by S. C. Schmidt*, et al.* (AIP Press, New York, 1994), pp. 1613-1616.

[7] F. Porsch and W. B. Holzapfel, Novel reentrant high pressure phase transition in lanthanum, *Phys. Rev. Lett.* **70**, 4087-4089 (1993).

[8] G. K. Samudrala, S. A. Thomas, J. M. Montgomery and Y. K. Vohra, High pressure phase transitions in the rare earth metal erbium to 151 GPa, *J. Phys.: Condens. Matter* **23**, 315701 (2011).

[9] G. K. Samudrala and Y. K. Vohra, Structural properties of lanthanides at ultra high pressure, in *Handbook on the Physics and Chemistry of Rare Earths*, edited by J. G. Bünzli and V. K. Pecharsky 2013), pp. 275-319.

[10] R. J. Husband, I. Loa, K. Munro and M. I. McMahon, The distorted-fcc phase of samarium, *J.Phys.: Conf. Ser.* **500**, 032009 (2014).

[11] R. Černý, Y. Filinchuk, H. Hagemann and K. Yvon, Magnesium borohydride: synthesis and crystal structure, *Angew. Chem. Inter. Ed.* **46**, 5765-5767

[12] R. S. Chellappa, M. Somayazulu, V. V. Struzhkin, T. Autrey and R. J. Hemley, Pressure-induced complexation of NH_3BH_3–H_2, *J. Chem. Phys.* 224515 (2009).

[13] Y. Song, New perspectives on potential hydrogen storage materials using high pressure, *Phys. Chem. Chem. Phys.* **15**, 14524–14547 (2013).

[14] R. G. Potter, M. Somayazulu, G. D. Cody and R. J. Hemley, High pressure equilibria of dimethylamine borane, dihydridobis(dimethylamine)boron(III) tetrahydridoborate(III), and hydrogen *J. Phys. Chem. C* **118**, 7280-7287 (2014).

[15] W. W. Zhan, Q. L. Zhu and Q. Xu, Dehydrogenation of ammonia borane by metal nanoparticle catalysts, *ACS Catalysis* **6**, 6892-6905 (2016).

[16] H. Liu, I. I. Naumov, Z. M. Geballe, M. Somayazulu, J. S. Tse and R. J. Hemley, Dynamics and superconductivity in compressed lanthanum superhydride, *Phys. Rev. B* **98**, 100102(R) (2018).

[17] L. J. van der Pauw, A method of measuring specific resistivity and Hall effect of discs of arbitrary shape, *Philips Res. Rep.* **13**, 1-9 (1958).

[18] J. P. Rush*, et al.*, Transport in bulk superconductors: a practical approach?, *IEEE Trans. Appl. Superconductivity* **26**, 1-4 (2016).

[19] R. J. Hemley, M. I. Eremets and H. K. Mao, Progress in experimental studies of insulator-metal transitions at multimegabar pressures, in *Frontiers of High Pressure Research II*, edited by H. D. Hochheimer*, et al.* (Kluwer, Amsterdam, 2002), pp. 201-216.

[20] M. I. Eremets, V. V. Viktor V. Struzhkin, H. K. Mao and R. J. Hemley, Exploring superconductivity in low-Z materials at megabar pressures, *Physica B* **329–333**, 1312–1316 (2003).
[21] A. G. Gavriliuk, A. A. Mironovich and V. V. Struzhkin, Miniature diamond anvil cell for broad range of high pressure measurements, *Rev. Sci. Instr.* **80**, 043906 (2009).
[22] H. Liu, I. I. Naumov, R. Hoffmann, N. W. Ashcroft and R. J. Hemley, Potential high-T_c superconducting lanthanum and yttrium hydrides at high pressure, *Proc. Natl. Acad. Sci. USA* **114**, 6990-6995 (2017).
[23] F. Peng, Y. Sun, C. J. Pickard, R. J. Needs, Q. Wu and Y. Ma, Hydrogen clathrate structures in rare earth hydrides at high pressures: Possible route to room-temperature superconductivity, *Phys. Rev. Lett.* **119**, 107001 (2017).
[24] A. P. Drozdov*, et al.*, Superconductivity at 215 K in lanthanum hydride at high pressures, arXiv:1808.07039
[25] Y. A. Timofeev, V. V. Struzhkin, R. J. Hemley, H. K. Mao and E. A. Gregoryanz, Improved techniques for measurement of superconductivity in diamond anvil cells by magnetic susceptibility, *Rev. Sci. Instrum.* **73**, 371-377 (2002).
[26] W. A. Grosshans, Y. K. Vohra and W. B. Holzapfel, Evidence for a soft phonon mode and a new structure in rare-earth metals under pressure, *Phys. Rev. Lett.* **49**, 1572 (1982).
[27] P. Loubeyre*, et al.*, X-ray diffraction and equation of state of hydrogen at megabar pressure, *Nature* **383**, 702-704 (1996).

Table S1: Experimental details for samples described in this study

Sample	Synthesis Pressure*	Cell Volume	Experimental Details
A	185(±5) GPa	32.0(±0.2) $Å^3$	Four-probe electrical conductivity
B	188(±5) GPa	31.1(±0.2) $Å^3$	Pseudo-four probe conductivity
C	175(±5) GPa	29.8(±0.2) $Å^3$	Pseudo-four probe conductivity
D	180(±5) GPa	14.5(±0.2) $Å^3$	Four-probe electrical conductivity (La)
E	182(±5) GPa	29.1(±0.2) $Å^3$	Low-temperature x-ray diffraction
F	177(±5) GPa	30.5(±0.5) $Å^3$	Four-probe electrical conductivity
G	179(±5) GPa	32.1(±0.5) $Å^3$	Pseudo-four probe conductivity

- Pressures determined from Pt x-ray diffraction.

‡ Sample synthesized from La + H_2; all other samples were synthesized from La + NH_3BH_3.

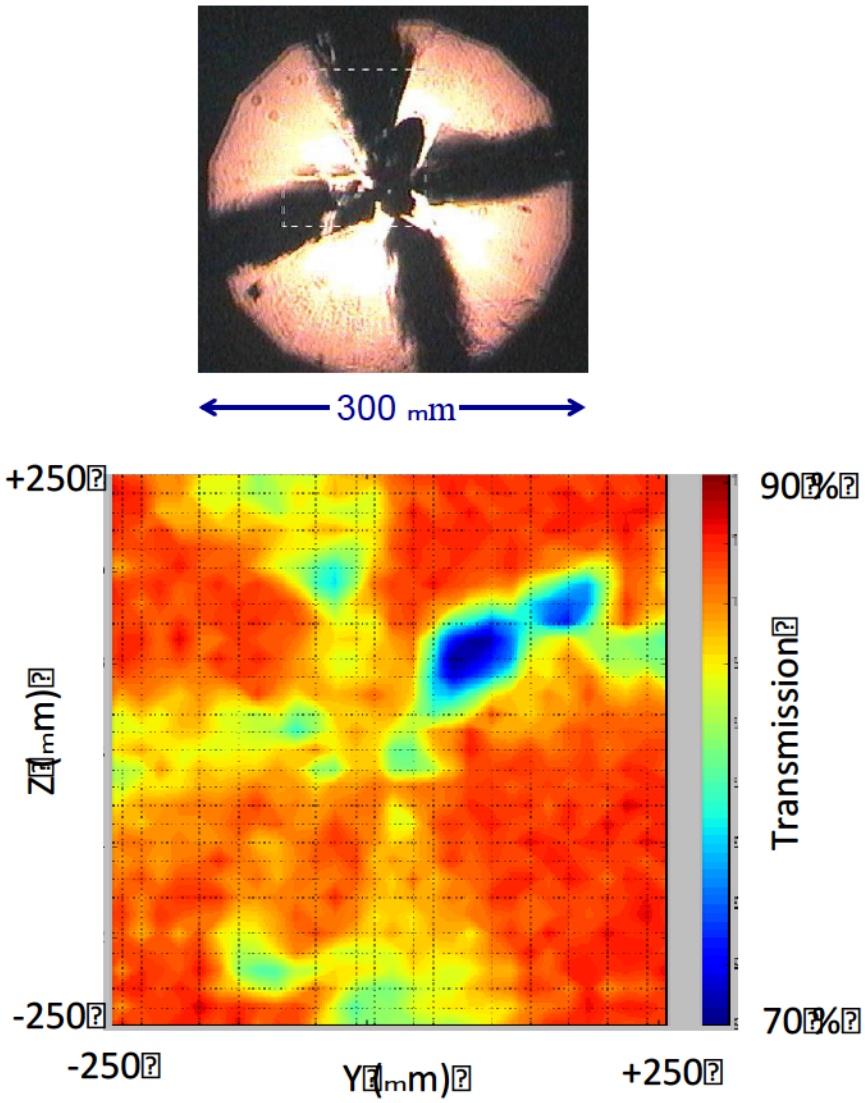

Figure S1. Top: Optical micrograph of sample A at 178 GPa after laser heating. Bottom: X-ray transmission radiograph of the assembly in a similar orientation, which shows the sample confined to the junction of the four Pt electrodes. The radiograph was reconstructed from contouring the transmitted x-ray intensity (λ = 0.4066 Å, or E = 30.492 keV) on a photodiode behind the sample that was rastered in perpendicular x and y directions in 2-μm steps.

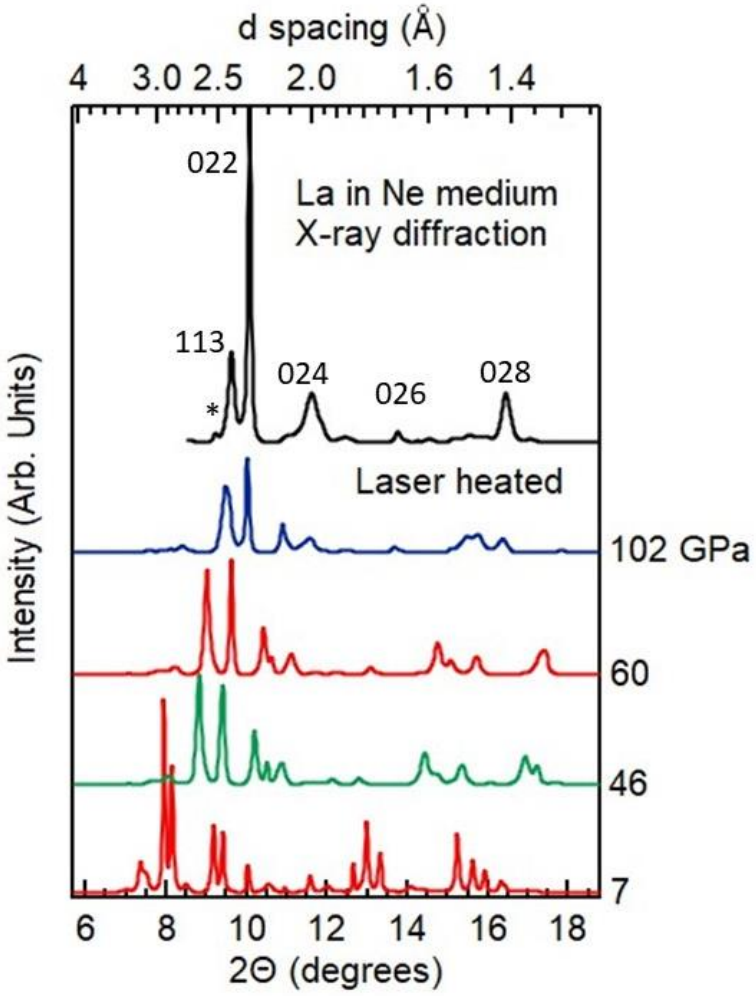

Figure S2. Representative x-ray diffraction data of La in a Ne medium as a function of pressure. The patterns were obtained at 16-ID-B of HPCAT using a focused x-ray beam at 0.4066 A. Diffraction data measured before and after laser heating at 102 GPa reveal changes in relative intensities of existing peaks, indicating no major change in structure from the *hR*24 phase which appears above 7 GPa (see Refs. [9,26]). The indicated indices are therefore based on the *hR*24 structure. The diffraction peak marked with an asterisk was observed in all runs and is assigned to an impurity. A detailed analysis of these data and the structure of La to 200 GPa will be presented elsewhere [5].

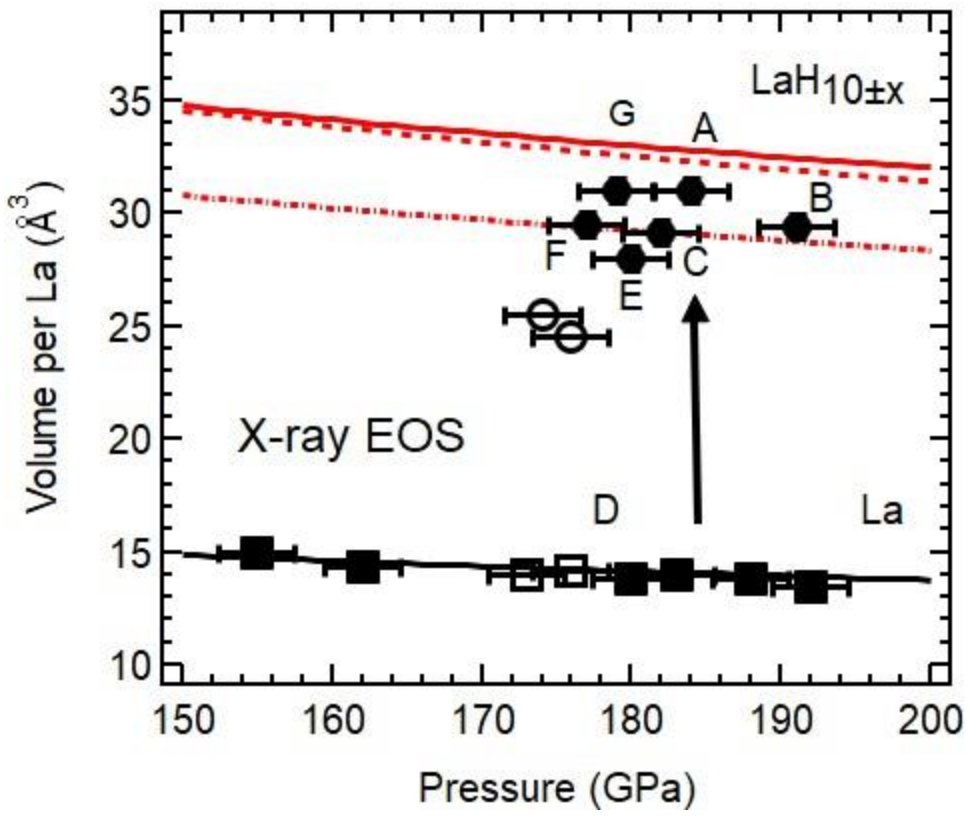

Figure S3. Observed volumes per La before and after conversion from La to $LaH_{10\pm x}$ for samples A-G for which electrical conductivity measurements were performed. All samples used NH_3BH_3 as the hydrogen source and were laser heated above 170 GPa as determined by a combination of diamond Raman [1] and Pt equation of state [2]. The x-ray determined *P-V* equations of state we reported earlier for $LaH_{10\pm x}$ and La are shown by the solid lines [4]. The predicted *P-V* curves for the assemblages La + $5H_2$ and La + $4H_2$ are plotted as the dashed and dash-dot lines, respectively, using the equations of state for La [4] and H_2 [27]. The arrow indicates the superhydride synthesis from La to $LaH_{10\pm x}$ (see also Ref. [14]). Open symbols correspond to samples that displayed no resistivity transition, including both unreacted La (sample D) and hydrides whose volumes lie below the La + $4H_2$ line.

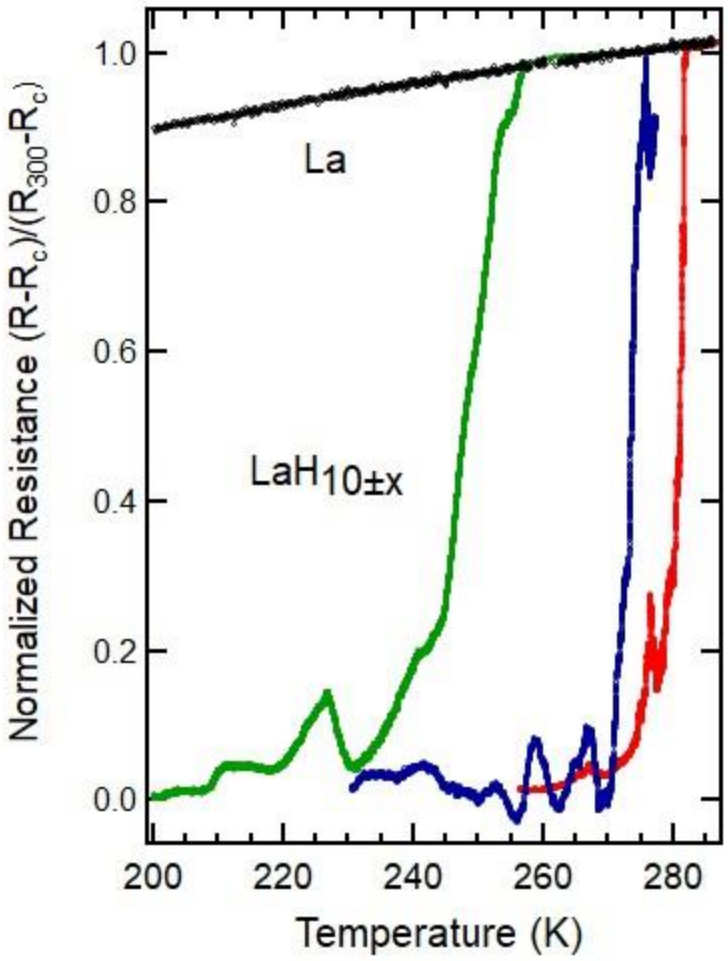

Figure S4. The normalized resistance [R(T)-R_c(T)) /(R(300 K)-R_c(T)] of $LaH_{10\pm x}$ (sample B) along with that of pure La (sample D) measured with a pseudo-four probe technique. The curves correspond to successive cooling and warming cycles where the pressure determined from the diamond Raman gauge [3] was 190 GPa (green), 195 GPa (blue) and 202 GPa (red) for the three warming and cooling. A correction for a linear contact resistance was applied (see text).

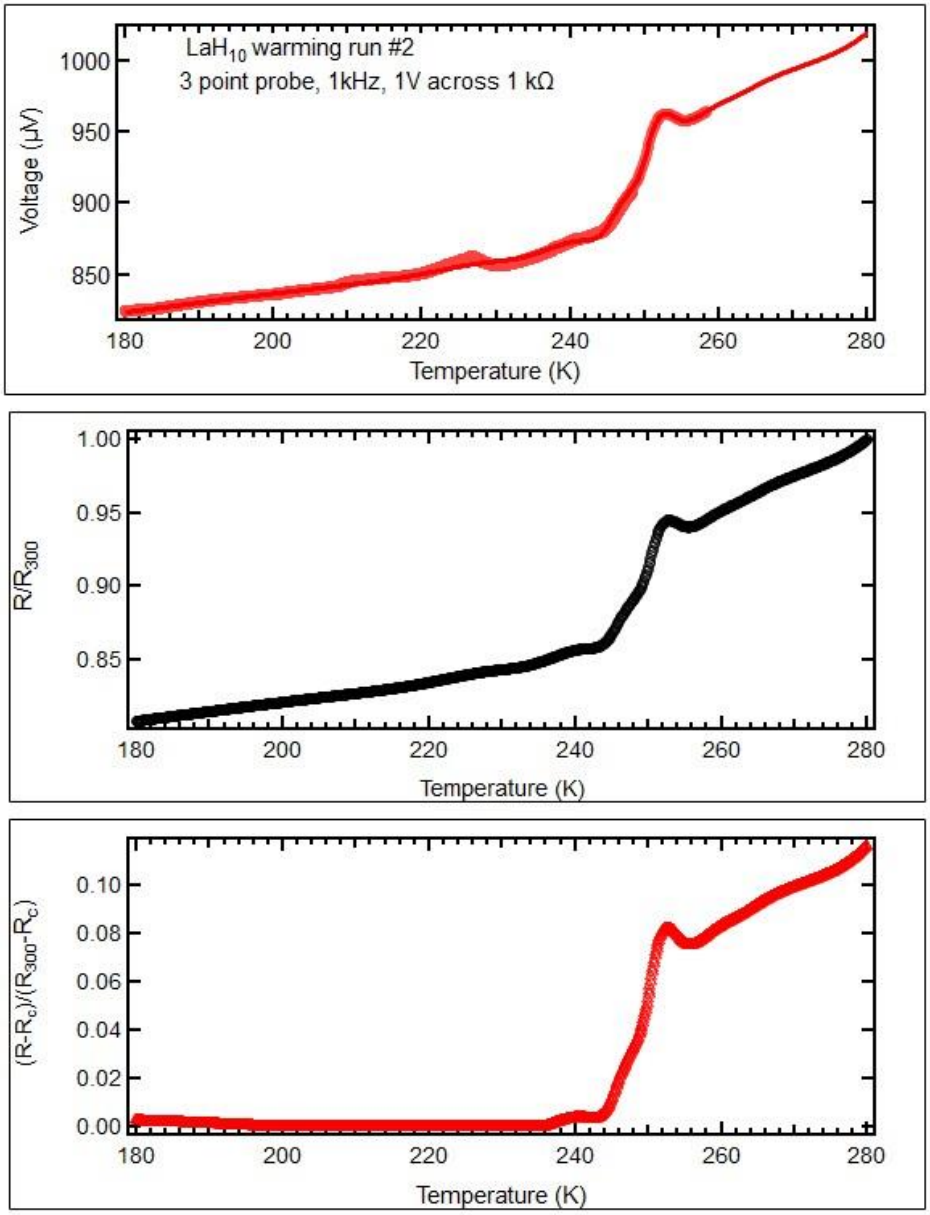

Figure S5. Selected resistance data obtained from the pseudo-four probe measurement of $LaH_{10\pm x}$ during a warming cycle from 150 K (sample B). The raw data shown in the top panel was normalized to the ambient resistance value (in this case, an extrapolated value) to obtain the relative resistance (R/R_{300}). These measurements were all made using a 1 V (peak-peak) sine wave input from a Rigol function generator applied to the sample using a 1 kΩ resistance to limit the load current as well as stabilize the applied load current. The output voltage was measured in a differential mode on a EG&G model 5209 lock-in amplifier with 1 kΩ isolating resistances across the input to the common ground.

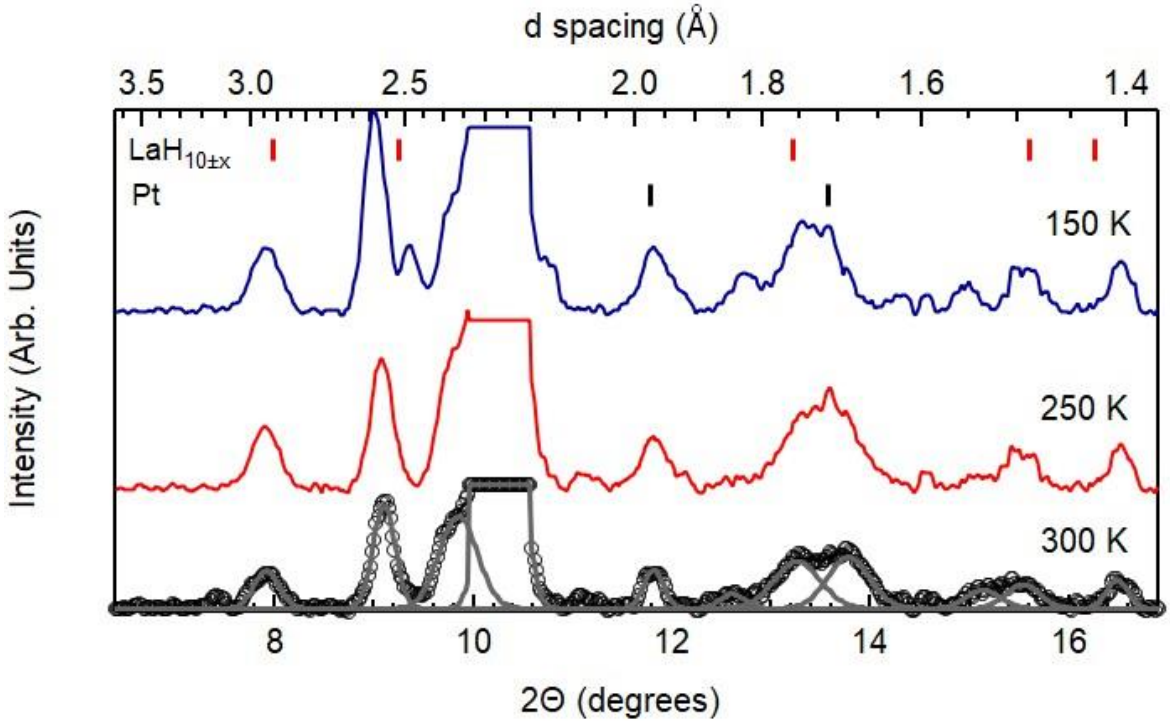

Figure S6. Representative powder x-ray diffraction patterns of $LaH_{10\pm x}$ (sample E) after synthesis at 182 GPa inside a cryostat before and during cooling. The positions of the principal peaks of $LaH_{10\pm x}$ and Pt are denoted by the red and black tick marks, respectively. The fit of the 300 K pattern is indicated. Additional peaks in all patterns, arise from background scattering from the sapphire window of the cryostat.

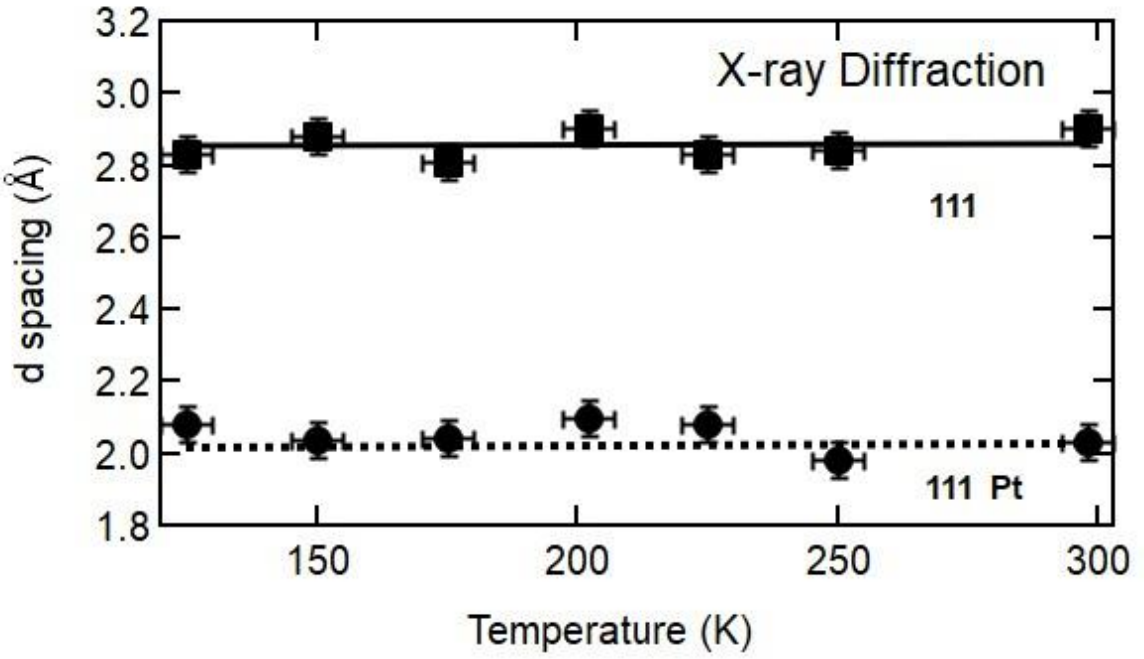

Figure S7. Observed d-spacings of $LaH_{10\pm x}$ and Pt as a function of temperature at 185 GPa taken from analysis of patterns such as those shown in Fig. S6. We show the d values of the two un-ambiguous and strong diffraction peaks from the representative diffraction patterns shown in Fig. S7. The spread in d spacings is due to the fact that the incident x-ray beam probed several parts of the sample. The lines are a guide to the eye and support our inference that there exists no anomalous volume change in $LaH_{10\pm x}$ in this temperature range.